

PAPER

# A tunable gelatin-hyaluronan dialdehyde/methacryloyl gelatin interpenetrating polymer network hydrogel for additive tissue manufacturing

To cite this article: Resmi Anand *et al* 2022 *Biomed. Mater.* **17** 045027

View the [article online](#) for updates and enhancements.

## You may also like

- [Coaxial extrusion bioprinting of 3D microfibrinous constructs with cell-favorable gelatin methacryloyl microenvironments](#)  
Wanjun Liu, Zhe Zhong, Ning Hu et al.
- [Effect of sterilization treatment on mechanical properties, biodegradation, bioactivity and printability of GelMA hydrogels](#)  
Muhammad Rizwan, Sarah W Chan, Patricia A Comeau et al.
- [Tunable metacrylated hyaluronic acid-based hybrid bioinks for stereolithography 3D bioprinting](#)  
Rafaeal Hossain Rakin, Hitendra Kumar, Ashna Rajeev et al.

BREATH<sup>®</sup>  
BIOPSY

## Breath Biopsy<sup>®</sup> OMNI

The most advanced, complete solution for global breath biomarker analysis

SEE WHAT OMNI  
CAN DO FOR YOU



Expert Study Design  
& Management



Robust Breath  
Collection



Reliable Sample  
Processing & Analysis



In-depth Data  
Analysis



Specialist Data  
Interpretation

# Biomedical Materials



## PAPER

# A tunable gelatin-hyaluronan dialdehyde/methacryloyl gelatin interpenetrating polymer network hydrogel for additive tissue manufacturing

Resmi Anand<sup>1,2,3,\*</sup>, Mehdi Salar Amoli<sup>2,4</sup>, An-Sofie Huysecom<sup>5</sup>, Paulo Alexandre Amorim<sup>1,2</sup>, Hannah Agten<sup>1,2</sup>, Liesbet Geris<sup>1,6,7</sup> and Veerle Bloemen<sup>1,2</sup>

<sup>1</sup> Prometheus, Division of Skeletal Tissue Engineering, KU Leuven, O&N 1, Herestraat 49, 3000 Leuven, Belgium

<sup>2</sup> Surface and Interface Engineered Materials (SIEM), Campus Group T, KU Leuven, Andreas Vesaliusstraat 13, 3000 Leuven, Belgium

<sup>3</sup> Inter University Centre for Biomedical Research and Super Speciality Hospital, Mahatma Gandhi University Campus at Thalappady, Kottayam, Kerala 686009, India

<sup>4</sup> Department of Imaging & Pathology/OMFS-IMPACT Research Group, Campus Sint-Rafaël, KU Leuven, Kapucijnenvoer 33, 3000 Leuven, Belgium

<sup>5</sup> Soft Matter, Rheology and Technology, Department of Chemical Engineering, KU Leuven, Leuven, Belgium

<sup>6</sup> Biomechanics Research Unit GIGA-R In Silico Medicine, Université de Liège, Quartier Hôpital, Avenue de l'Hôpital 11, Liège, Belgium

<sup>7</sup> Biomechanics Section, KU Leuven, Celestijnenlaan 300C (2419), Leuven, Belgium

\* Author to whom any correspondence should be addressed.

E-mail: [resmi25@gmail.com](mailto:resmi25@gmail.com)

**Keywords:** bioprinting, interpenetrating network, methacryloyl gelatin, hyaluronic acid, rheology, bioink

## Abstract

Methacryloyl gelatin (GelMA) is a versatile material for bioprinting because of its tunable physical properties and inherent bioactivity. Bioprinting of GelMA is often met with challenges such as lower viscosity of GelMA inks due to higher methacryloyl substitution and longer physical gelation time at room temperature. In this study, a tunable interpenetrating polymer network (IPN) hydrogel was prepared from gelatin-hyaluronan dialdehyde (Gel-HDA) Schiff's polymer, and 100% methacrylamide substituted GelMA for biofabrication through extrusion based bioprinting. Temperature sweep rheology measurements show a higher sol-gel transition temperature for IPN (30 °C) compared to gold standard GelMA (27 °C). Furthermore, to determine the tunability of the IPN hydrogel, several IPN samples were prepared by combining different ratios of Gel-HDA and GelMA achieving a compressive modulus ranging from  $20.6 \pm 2.48$  KPa to  $116.7 \pm 14.80$  KPa. Our results showed that the mechanical properties and printability at room temperature could be tuned by adjusting the ratios of GelMA and Gel-HDA. To evaluate cell response to the material, MC3T3-E1 mouse pre-osteoblast cells were embedded in hydrogels and 3D-printed, demonstrating excellent cell viability and proliferation after 10 d of 3D *in vitro* culture, making the IPN an interesting bioink for the fabrication of 3D constructs for tissue engineering applications.

## 1. Introduction

3D bioprinting is an interesting biofabrication technology that enables the precise positioning of cells, bioactive molecules and supporting matrix in 3D to construct functional tissues/organ analogues for biomedical applications [1]. The process of bioprinting often involves layer-by-layer deposition of a mixture of supporting matrix with cells, called a 'bioink' [2]. Different bioprinting strategies have been developed in the last decades including stereolithography, inkjet, extrusion, and laser-assisted printing. Among these, extrusion-based bioprinting is one of the most widely

used printing modalities due to its high affordability, along with the versatility of the printing technique with different cell types and biomaterials, allowing fabrication of complex structures [3, 4].

Among different materials used in bioinks, hydrogels are considered as a superior class of materials due to their excellent biocompatibility and similarity to the natural extracellular matrix (ECM) [5, 6]. Hydrogels derived from natural and synthetic polymers such as collagen, gelatin, methacryloyl gelatin (GelMA), and polyethylene glycol diacrylate have been used widely in bioink formulations to engineer analogues of different tissues [2]. Among these, GelMA is a

widely used candidate for the development of novel bioinks due to its high biocompatibility, presence of cell supporting arginyl-glycyl-aspartic acid (RGD) (Arg-Gly-Asp) peptides, tunable mechanical properties and the possibility of enzymatic degradation caused by the presence of matrix metalloproteinase sensitive moieties [7, 8]. However, the highly elastic property of bioinks made of low methacryloyl substituted gelatin, along with the possibility of clog formation inside the printing nozzles, make the extrusion-based printing of GelMA at room temperature challenging [9, 10]. Still, the direct printing of GelMA can be achieved by adjusting the parameters [11] such as altering the concentration of GelMA ink, using a lower methacryloyl substituted GelMA, pre-condition the GelMA ink at lower temperature to obtain required viscosity for printing, using a temperature-controlled nozzle/platform, enzyme-induced controlled crosslinking of GelMA and modifying the rheological properties of GelMA by preparing polymer blends or interpenetrating polymer networks (IPNs) [7, 12–14]. IPN hydrogels are systems composed of two or more polymer networks, in which the individual polymer networks are physically entangled with each other while being cross-linked only with themselves, leading to exhibition of both individual and synergistic properties of the polymer components in the hydrogel [15]. A suitable IPN hydrogel for tissue engineering should allow cell attachment and proliferation, should possess mechanical properties matching the target tissue and should have an appropriate degradation profile. While IPN hydrogels have been studied extensively for tissue engineering and drug delivery applications [16], reports of IPN use as bioinks are still limited.

Hyaluronic acid (HA) is a linear polysaccharide consisting of D-glucuronic acid and N-acetyl-D-glucosamine repeating units, which is ubiquitous in the human body [17]. It is the major glycosaminoglycan of the ECM and possesses excellent biocompatibility, biodegradability, and non-immunogenicity. Furthermore, HA can interact with cell surface receptors, CD 44 and CD 168 to regulate tissue architectures, cell adhesion, migration, and proliferation [18, 19]. Consequently, it is extensively employed in tissue engineering applications [20]. However, the clinical tissue engineering application of unmodified HA is limited due to its high water solubility leading to poor mechanical integrity in aqueous environments, a challenge that could possibly be addressed by using IPN hydrogels based on modified gelatin and HA. In this regard, Pescosolido *et al*, reported a bioprinted semi-IPN consisting of hydroxyethyl-methacrylate-derivatized dextran and HA [21]. However, the mere blending of HA with hydroxyethyl-methacrylate-derivatized dextran may compromise the residence time of HA because of its higher hydrophilicity. Furthermore, Lou *et al*, reported a stress relaxing IPN hydrogel synthesized by

crosslinking HA with collagen I through dynamic covalent bonds. Dynamic covalent crosslinking of HA reportedly led to global stress relaxation of the IPN hydrogel, promoting cell spreading [22]. Hence, considering the advantages and limitations of natural polysaccharide HA and gelatin for clinical tissue engineering applications, we hypothesized that modification of HA by dynamic covalent linking to gelatin, and further stabilization of the HA-gelatin by intercalating with GelMA to form an IPN network, can be an innovative approach for the development of gelatin and hyaluronic acid-based bioinks, aimed at the fabrication of 3D constructs for tissue engineering.

Herein, we report the synthesis of a 100% methacrylamide substituted gelatin using a stepwise pH adjustment method. We also report the synthesis and bioprinting of a Gel-HDA/GelMA IPN bioink with lower sol-gel transition time at room temperature and tunable mechanical properties for diverse bioprinting applications.

## 2. Experimental

### 2.1. Materials

Gelatin from porcine skin (type A, bloom 300), methacrylic anhydride (MAA) (94%), HA sodium salt ( $M_w$  1.5–1.8  $\times 10^6$ ), sodium (meta)periodate (99%) and lithium phenyl-2,4,6-trimethylbenzoylphosphinate (LAP) were purchased from Sigma Aldrich (St. Louis, MO, USA). Dulbecco's modified Eagle's medium (DMEM) and antibiotic-antimycotic were obtained from Gibco, Life Technologies (USA).

MC3T3-E1 cells obtained from mouse calvaria was purchased from Sigma Aldrich (Belgium), and were cultured in DMEM with 10% fetal bovine serum (Gibco, USA) and 1% antibiotic-antimycotic at 37 °C with a humidified 5% CO<sub>2</sub> atmosphere. Live/dead™ cell viability assay kit was purchased from Invitrogen, ThermoFisher Scientific (USA). MTS CellTiter® 96 aqueous one solution cell proliferation assay kit was purchased from Promega (Belgium).

### 2.2. The preparation of gelatin-hyaluronan dialdehyde/methacryloyl gelatin (Gel-HDA/GelMA) IPN hydrogel

#### 2.2.1. Synthesis of hyaluronan dialdehyde (HDA)

HDA was prepared according to a previously reported procedure [23]. Briefly, HA (1 g, 2.5 mmol) was dissolved in 100 ml deionized (DI) water by stirring overnight at room temperature. Sodium (meta)periodate (320 mg) was dissolved in 5 ml DI water, added to the HA solution dropwise, and stirred for 6 h at 25 °C in a dark environment. Next, the unreacted sodium meta periodate was quenched by adding a few drops of ethylene glycol. The mixture was dialyzed in a 12 000 Da dialysis tubing (Sigma Aldrich, USA) against water at 25 °C for 5 days to remove traces of periodate and low molecular weight

polymers. The solution was then lyophilized to obtain an oxidized product as a white solid sponge. The material was stored at  $-20^{\circ}\text{C}$  for further use.

#### 2.2.2. Synthesis of gelatin-hyaluronan dialdehyde (Gel-HDA) Schiff's polymer

Gelatin (10% (w/v), phosphate buffer saline (PBS), pH 7.4) was mixed with HDA (10% (w/v), in PBS) with a volume ratio of 4:1 and incubated at  $37^{\circ}\text{C}$  for 12 h to obtain Gel-HDA Schiff's base gel.

#### 2.2.3. Synthesis of methacryloyl gelatin (GelMA)

The synthesis of GelMA was performed by modifying a procedure reported in the literature [24]. Briefly, 200 ml gelatin type A solution (10% (w/v)) was prepared in a carbonate-bicarbonate buffer (0.25 M, pH 9.5) by stirring at  $40^{\circ}\text{C}$  for 12 h. To this solution, MAA (3 ml) was added slowly. The pH of the reaction was maintained above 7 by adding drops of NaOH (5 N). The reaction occurred immediately upon the addition of MAA and was confirmed by a decrease in pH due to the release of methacrylic acid by-product. The stirring was continued for another 2 h to ensure the maximum degree of methacryloyl substitution. Next, the reaction mixture was cooled to room temperature and was kept for dialysis (molecular weight cut off 12 000 Da, Sigma Aldrich, USA) against DI water for 5 days at room temperature. Eventually, the mixture was lyophilized to obtain the product GelMA as a white solid sponge. The material was stored at  $-20^{\circ}\text{C}$  for further use.

#### 2.2.4. Preparation of Gel-HDA/GelMA IPN hydrogel

GelMA 10% (w/v) was prepared by dissolving GelMA in PBS (pH 7.4). IPN was prepared by mixing equal volumes of Gel-HDA Schiff's polymer (10% (w/v)) and GelMA (10% (w/v)). LAP photoinitiator ( $0.1\text{ mg ml}^{-1}$ ) was mixed and exposed to 365 nm UV light for 1 min, after 3D printing/bioprinting to form the IPN hydrogels.

### 2.3. Structural characterization

$^1\text{H}$  nuclear magnetic resonance (NMR) spectra of gelatin, GelMA, hyaluronic acid, HDA and Gel-HDA were taken on a Bruker Avance III, 400 MHz spectrometer. The fourier-transform infrared spectroscopy (FTIR)-attenuated total reflection (ATR) spectra of gelatin, HDA and Gel-HDA Schiff's polymer were recorded in the range of  $4000\text{--}400\text{ cm}^{-1}$  using Bruker Vertex 70 FTIR spectrometer with diamond ATR accessory.

### 2.4. Evaluation of the degree of methacryloyl substitution

The degree of methacryloyl substitution in gelatin was calculated from  $^1\text{H}$  NMR spectra (by integrating the peak 2.8 ppm).

### 2.5. Mechanical properties

To study the effect of Gel-HDA concentrations on the mechanical properties of GelMA, five different

IPN samples consisting of different concentrations of Gel-HDA and GelMA, with the total polymer concentration fixed at 10% (w/v) were prepared. The different IPN samples were IPN1 (Gel-HDA 1% (w/v) + GelMA 9% (w/v)), IPN2 (Gel-HDA 3% (w/v) + GelMA 7% (w/v)), IPN3 (Gel-HDA 5% (w/v) + GelMA 5% (w/v)), IPN4 (Gel-HDA 7% (w/v) + GelMA 3% (w/v)) and IPN5 (Gel-HDA 9% (w/v) + GelMA 1% (w/v)). GelMA 10% (w/v) was used as the reference sample. GelMA and IPN precursors containing  $0.1\text{ mg ml}^{-1}$  LAP were pipetted into a cylindrical hollow mould, placed on a glass slide and exposed to  $6.9\text{ mW cm}^{-2}$  UV light (365 nm) for 60 s. Samples (10 mm height, 5.4 mm diameter) were detached from the mould and tested immediately at a rate of  $1\text{ mm s}^{-1}$  strain at room temperature on an Instron 5542 mechanical tester equipped with 100 N load cell. The stress-strain curve was calculated from the load-displacement data by normalizing to cross-sectional area and height of the sample. The compressive moduli were calculated by taking the slope of the linear region corresponding with 10% strain. Each point represents the mean  $\pm$  standard deviation ( $n = 5$ ).

### 2.6. Rheology

A stress-controlled shear rheometer (Anton Paar MCR501) equipped with a parallel plate test geometry of 50 mm and a solvent trap was used in small-amplitude oscillatory shear mode. To ensure that the physical structure of the hydrogels was formed between the rheometer plate and test geometry, each sample was loaded onto the rheometer plate in the liquid state ( $40^{\circ}\text{C}$ ) and the test geometry was lowered to a measuring gap of  $500\text{ }\mu\text{m}$  while still a liquid sample. A waiting time of 200 s was applied to ensure thermal equilibrium. Strain-amplitude sweep measurements were performed in the range of 0.1%–100% strain at  $20^{\circ}\text{C}$  and an angular frequency of  $10\text{ rad s}^{-1}$  to determine the linear viscoelastic envelope. A strain of 1% was verified to be in the linear regime. Time sweep tests at 1% strain and  $10\text{ rad s}^{-1}$  over a period of 2 h were performed to determine shear equilibrium modulus of the final hydrogels. The angular frequency sweep test was performed in the linear viscoelastic region at 1% strain,  $20^{\circ}\text{C}$ , and  $0.1\text{--}100\text{ rad s}^{-1}$  to obtain the mechanical spectrum of the hydrogels. Temperature sweep measurements at a heating rate of  $1^{\circ}\text{C min}^{-1}$  from  $10^{\circ}\text{C}$  to  $40^{\circ}\text{C}$  using 1% strain and  $10\text{ rad s}^{-1}$  were performed to find the sol-gel transition temperature of the hydrogels (GelMA and IPN (IPN3, Gel-HDA 5% (w/v) + GelMA 5% (w/v))).

### 2.7. Swelling and degradation study

The swelling and degradation percentages of GelMA and IPN (IPN3, Gel-HDA 5% (w/v) + GelMA 5% (w/v)) hydrogels were measured gravimetrically. Briefly, cylindrical-shaped ( $5\text{ mm height} \times 5.4\text{ mm}$



diameter) photocrosslinked (1 min, 365 nm) IPN and GelMA hydrogel samples were immersed in PBS (pH 7.4) at 37 °C under static conditions. At different time points, the PBS-soaked samples were taken out and reweighed. The swelling percentage was calculated according to equation (1):

$$\text{Swelling (\%)} = \frac{W_t - W_0}{W_0} \times 100 (\%) \quad (1)$$

where  $W_0$  is the initial mass of the dried sample and  $W_t$  mass of the swollen sample at a given time point  $t$ .

The degradation analysis was performed in DMEM at 37 °C. At different time points, DMEM-soaked samples were taken out, freeze dried and reweighed. The percentage of degradation was calculated following equation (2):

$$\text{Degradation (\%)} = \frac{W_0 - W_{tdry}}{W_0} \times 100 (\%) \quad (2)$$

where  $W_0$  is the initial mass of the dried sample and  $W_{tdry}$  is the mass of the freeze dried sample at a given time point  $t$ .

### 2.8. 3D printing and bioprinting

A 3D bioprinter (3DDiscovery™ Evolution, RegenHU, Switzerland) equipped with a piston-driven cartridge was used to print GelMA and IPN (IPN3, Gel-HDA 5% (w/v) + GelMA 5% (w/v)) hydrogels. The hydrogel precursors were loaded into a sterile cartridge. To print at room temperature IPN polymer precursor along with LAP photoinitiator with and without cells were incubated at room temperature for 20 min. The GelMA polymer precursor was incubated in the fridge at 4 °C for 20 min for physical gelation. The printing was performed using 27 G nozzles at room temperature (~21 °C).

The quantification of printability and optimum printing parameters was performed based on a previously reported method [25]. For this purpose, square-shaped constructs (one-layer, dimension: 1 cm × 1 cm, three replicates) were printed. The printability (Pr) was determined based on the nature of the square-shaped prints. Ideally, the extruded filament would produce a smooth surface with constant width resulting in square-shaped holes, otherwise, the holes tend to form circular geometry. Calculation of the printability was based on the circularity ( $C$ ) of the square-shaped holes:

$$\text{ie., } C = 4\pi AL^{-2} \quad (3)$$

where  $L$  is the perimeter and  $A$  is the area.

In a perfect circle condition,  $C = 1$ . The circularity ( $C$ ) for square-shaped constructs is  $\pi/4$ , and hence the printability parameter (Pr) value can be calculated by using equation (4) [25]:

$$\text{Pr} = \frac{\pi}{4} \cdot \frac{1}{C} = \frac{L^2}{16A} \quad (4)$$

Therefore, for a perfect printability, the Pr value must be 1.

To determine the printability value for each combination of printing parameters, the microscopic images of the printed constructs were analyzed ([www.sketchandcalc.com/](http://www.sketchandcalc.com/)) to measure the perimeter and enclosed area of the printed constructs.

Based on the above evaluation of printability, the printing parameters were determined for both GelMA and IPN samples and 3D printed constructs having different shapes (grid, stacked hollow cylinder, and alphabets) were printed. Images of the 3D printed constructs were taken for the qualitative evaluation of the shape fidelity.

For bioprinting, a cell density of 1 million cells  $\text{ml}^{-1}$  was prepared by gently mixing GelMA and IPN (IPN3, Gel-HDA 5% (w/v) + GelMA 5% (w/v)) samples incubated at 37 °C with the required amount of MC3T3 cell pellets. The cell-laden bioinks were loaded into a cartridge and kept at room temperature for 20 min to attain physical gelation. The bioprinted constructs were printed on a six-well plate, photocrosslinked (1 min) and immersed in DMEM (5 ml) supplemented with 10% fetal bovine serum and 1% antibiotic-antimycotic, and incubated at 37 °C in a humidified  $\text{CO}_2$  (5%) incubator.

### 2.9. Surface morphology by scanning electron microscopy (SEM)

The surface morphology of the 3D printed grid-shaped samples (10 × 10 × 0.4 mm) was analyzed by SEM (Philips XL30 FEG) after chemical crosslinking. The 3D printed samples were frozen at −80 °C, lyophilized and dried samples were sputtered with platinum at a thickness of 5 nm using Q 150 T S, Pt/Pd sputter coater before imaging. SEM images were used to analyse average pore size by measuring the pore area of ten pores using FIJI software [26], and calculating the diameter by assuming circular pores.

### 2.10. In vitro cell viability

The viability of the MC3T3 cells encapsulated ( $1 \times 10^6$  cells  $\text{ml}^{-1}$ ) within the bioprinted IPN hydrogel (IPN3, Gel-HDA 5% (w/v) + GelMA 5% (w/v)) construct was evaluated using a LIVE/DEAD™ Viability/Cytotoxicity Kit (Invitrogen, Life Technologies, USA) after 1, 3 and 10 days post-printing following the manufacturers' protocol. Images were taken using fluorescence microscopy (Olympus IX83 inverted microscope, Belgium).

### 2.11. Cell proliferation study

MTS colorimetric assay was used to analyze the proliferation of MC3T3 pre-osteoblasts encapsulated within the bioprinted GelMA and IPN (IPN3, Gel-HDA 5% (w/v) + GelMA 5% (w/v)) constructs. To determine the cell viability, 60  $\mu\text{l}$  of MTS dye (CellTiter® 96Aqueous One Solution Cell Proliferation Assay kit) was added to 300  $\mu\text{l}$  MEM in a 48-well plate

and incubated at 37 °C for 3 h. Next, 100 µl of the solution from each well was transferred into a 96-well plate and the absorbance at 490 nm was measured using a microplate reader. The optical density (OD) values for cell-encapsulated bioprinted GelMA and IPN hydrogels were recorded as OD<sub>sample</sub> and the value of corresponding blank control group (3D printed GelMA and IPN without cells) was measured as OD<sub>blank</sub>. The actual OD value, which reflected the metabolic activity of cells, was calculated by subtraction of the blank readings from the sample readings.

### 2.12. Statistical analysis

Two-way ANOVA and multiple comparisons tests were performed using GraphPad Prism (version 8.0.0 for Windows, GraphPad Software, San Diego, California USA, [www.graphpad.com](http://www.graphpad.com)) for comparing the experimental groups. All values provided are expressed as the mean ± standard deviation of five replicates. *p* value <0.05 was considered as statistically significant.

## 3. Results and discussion

### 3.1. Synthesis and structural characterization of Gel-HDA/GelMA IPN hydrogel

The design of the material allows stabilization of the construct by dual crosslinking chemistries, including physical crosslinking and chemical crosslinking through methacryloyl groups. By chemically linking HA into gelatin, the less stable HA can be stabilized in the network. This was achieved by dynamic covalent linkage of free amino groups in Gel-HDA through Schiff's base chemistry. For this purpose, HA was oxidized to HDA by the sodium meta periodate oxidation method [27]. The presence of sodium meta periodate opens the sugar ring of HA to form linear chains with dialdehydes, resulting in the pale yellow coloration of the oxidized product. The oxidized product, HDA, was then mixed with gelatin to form Gel-HDA Schiff's base polymer through imine linkage. The Gel-HDA polymer network was selected as the primary network for the preparation of the IPN.

GelMA with 100% methacrylamide substitution was synthesized for the first time from gelatin type A by stepwise pH adjustment through slight modifications on the method reported by [24] (scheme 1(A)). The isoelectric point of type A gelatin is between 8 and 9, meaning that at this pH the lysine groups of the protein remain neutral and primary amine groups on lysine will be available for reaction with MAA. None of the –OH groups were methacrylated, as the pH of the reaction mixture was always kept above 7 using NaOH (5 N) drops.

The Gel-HDA/GelMA IPN was synthesized by intercalating GelMA polymer precursor into Gel-HDA polymer network, followed by chemical crosslinking of GelMA in the presence of LAP upon UV exposure. The complete functionalization of free

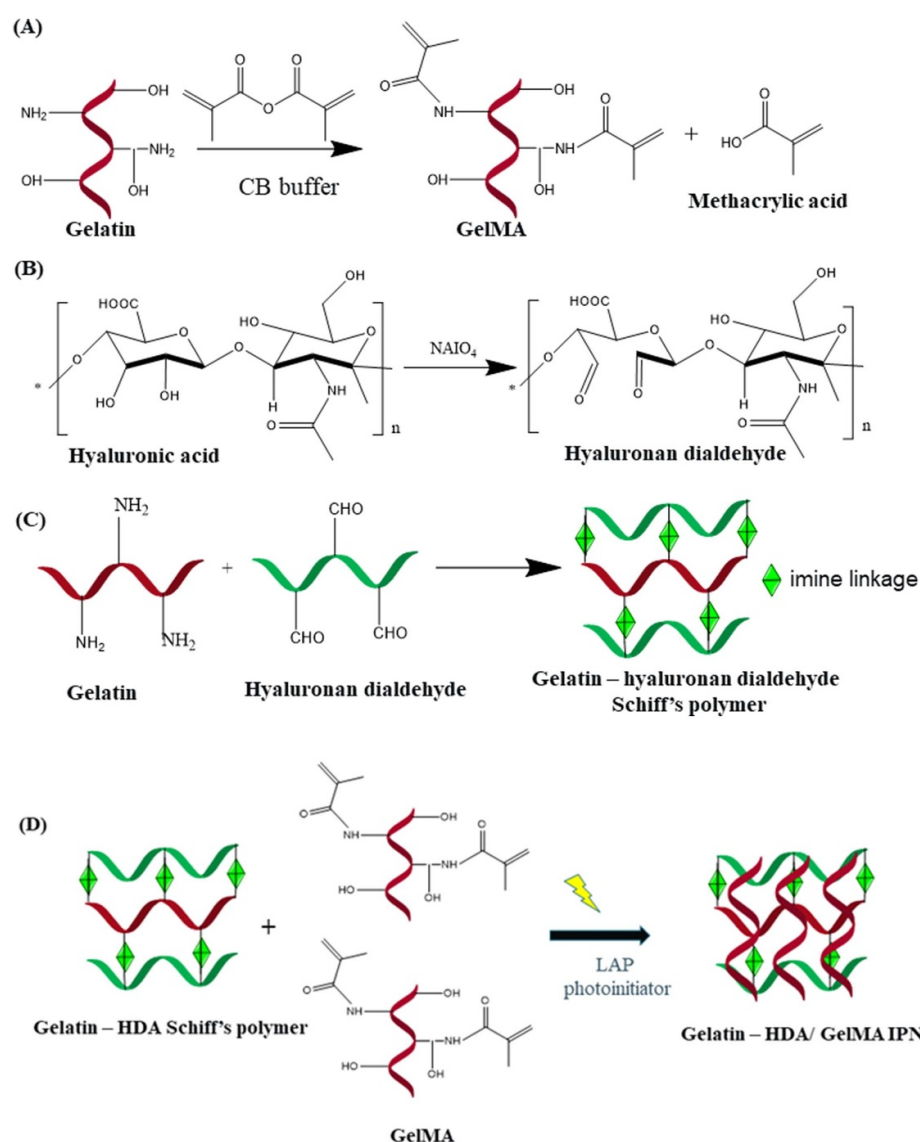
amine groups, present on the lysine protein, by methacryloyl group is important for preparation of the IPN network, as these groups are the reaction site for both MAA and hyaluronan dialdehyde. Hence, introducing the need for 100% methacryloyl substituted gelatin to avoid a crosslinking reaction between GelMA and HDA. Consequently, further tuning of degradation and physical properties of the IPN would be possible only through adjusting the concentration of primary and secondary networks. Moreover, 100% methacryloyl functionalization decreases the elasticity by hindering hydrogen binding sites of GelMA, which helps in reducing the clog formation inside the nozzle while printing. A schematic representation for the synthesis of Gel-HDA/GelMA IPN is shown in scheme 1.

Additionally, in case of presence of any uncross-linked HA and gelatin, they may be entangled in GelMA, which would assist cell migration within the construct via binding through the CD 44 receptor of HA [28, 29] and RGD integrin-binding sites of GelMA. Moreover, the IPN structure may provide synergistic properties of individual polymer networks leading to a better control over the material properties.

### 3.2. Characterization of Gel-HDA/GelMA IPN

Figure 1(A) shows the structural characterization of GelMA and gelatin by recording <sup>1</sup>H NMR spectroscopy. The disappearance of methylene lysine proton at 2.8 ppm clearly indicates the conjugation of MAA with the lysine moiety of gelatin. The acrylic proton of the methacrylamide graft was observed at 5.5 ppm (peak a + b) and methyl protons of methacrylamide were observed at 1.9 ppm (peak c) indicating the functionalization of MAA on gelatin [24]. Interestingly, no methacrylate group (methacryloyl substitution on the –OH group) is formed due to this modification. The degree of methacryloyl substitution was calculated from the <sup>1</sup>H NMR spectrum (integrating the peak at 2.8 ppm). The complete disappearance of methylene lysine proton at 2.8 ppm indicated 100% functionalization of methacryloyl groups on the lysine moiety.

Figure 1(B) presents the FTIR spectra of gelatin, HA, HDA, and Gel-HDA Schiff's hydrogel. HA has a disaccharide structure composed of D-glucuronic acid and N-acetyl glucosamine, resulting in the characteristic stretching bands for the hydroxyl groups at 3286 cm<sup>-1</sup> and the –CH<sub>2</sub> stretching vibration at 2900 cm<sup>-1</sup> [30]. Compared to HA, a new peak that appeared at 1733 cm<sup>-1</sup> of HDA spectra corresponds to the C=O stretching [31], confirming the introduction of the aldehyde groups into HA by periodate oxidation method. The FTIR spectrum of gelatin shows its characteristic bands at 1629 cm<sup>-1</sup> (amide I, C=O stretching), 1528 cm<sup>-1</sup> (amide II, a combination of CN stretch and NH deformation), 1234 cm<sup>-1</sup> (amide III, a combination of CN stretching, NH



**Scheme 1.** Schematic representation of (A) the synthesis of methacryloyl gelatin (GelMA) (B) periodate oxidation of hyaluronic acid to hyaluronan dialdehyde (C) preparation of gelatin-hyaluronan dialdehyde (Gel-HDA) Schiff's polymer and (D) synthesis of a Gelatin-HDA/GelMA IPN hydrogel.

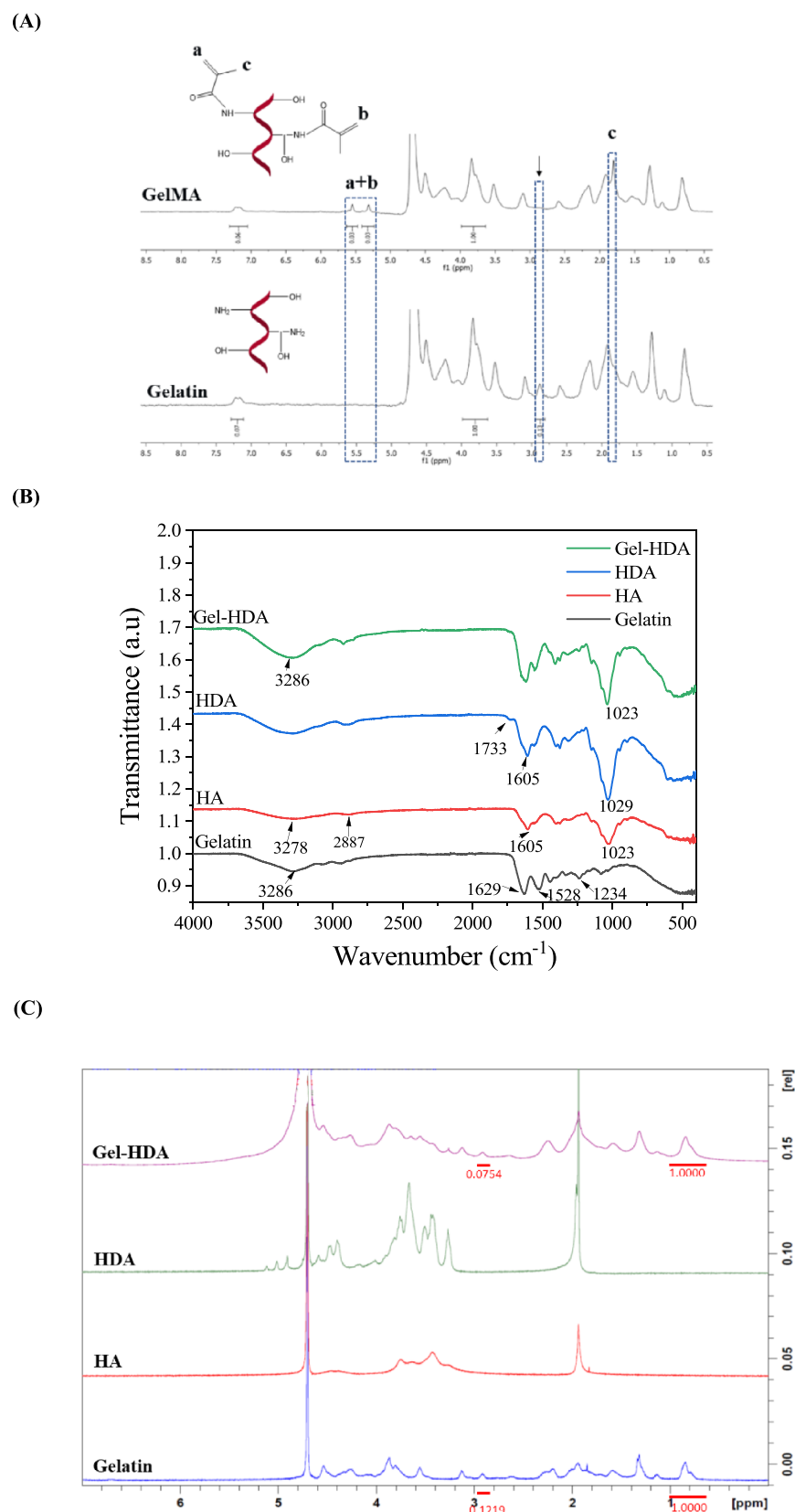
bending and  $\text{CH}_2$  wagging). The broad absorption band at  $3286\text{ cm}^{-1}$  is arising from  $-\text{OH}$  and  $\text{NH}$  stretching [32]. The FTIR spectra of gelatin cross-linked HDA (Gel-HDA) Schiff's base sample show a decrease in the intensity of amide II band indicating that the amino groups are involved in the cross-linking reaction to form Gel-HDA Schiff's base. Also, the characteristic band of  $\text{C}=\text{O}$  stretching vibration at  $1733\text{ cm}^{-1}$  disappeared as a result of the consumption of aldehyde groups through the crosslinking of HDA and gelatin.

HDA was also characterized by  $^1\text{H}$  NMR spectroscopy (figure 1(C)). The multiplet peak at 1.9 ppm corresponds to acetamide protons ( $\text{NH}-\text{CO}-\text{CH}_3$ ). The peaks from 3.2 to 3.8 ppm is ascribed to the proton of sugar unit ( $\text{CH}-\text{O}$  and  $\text{CH}_2-\text{O}$ ). The peak (multiplet) centered at 4.4 ppm corresponds to the anomeric proton ( $\text{OCH}-\text{O}$ ) from the glucose unit. The multiplet peak at 5.0 and 5.1 ppm corresponds

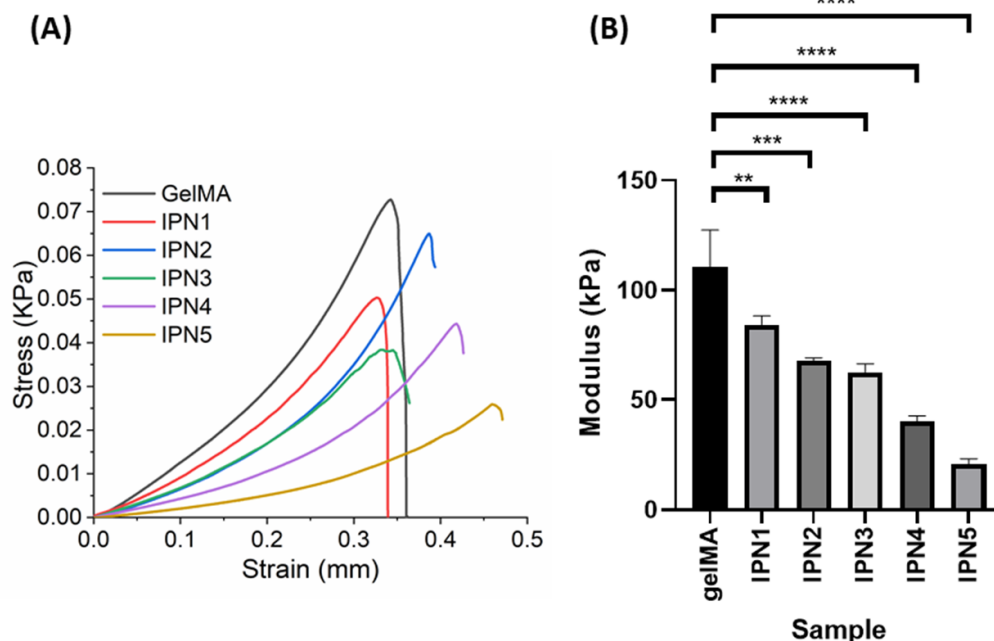
to the hemiacetal formation of aldehyde and adjacent hydroxyl groups. In Gel-HDA, the disappearance of hemiacetal proton (5.0 and 5.1 ppm) and decrease in intensity of free amine group (2.9 ppm) confirm the conjugation of HDA and gelatin.

### 3.3. Mechanical properties

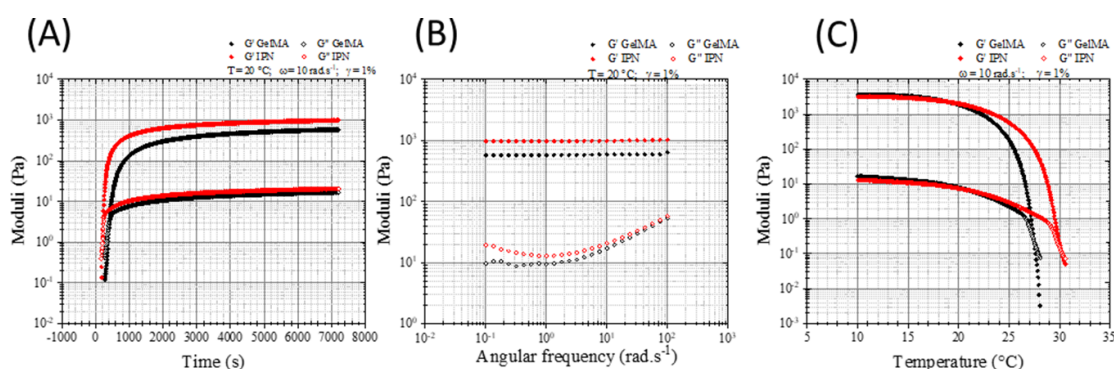
GelMA-based hydrogels with tunable mechanical properties and methacryloyl crosslinking densities could be interesting for diverse tissue engineering applications, due to the wide range of mechanical requirements for different applications, and the fact that the mechanical properties of the hydrogels and crosslinking density can regulate the behaviour of cells in terms of cell proliferation, migration and differentiation [10]. In order to investigate the effect of Gel-HDA network in the mechanical properties of GelMA, IPN samples with different Gel-HDA and GelMA concentrations were prepared.



**Figure 1.** (A)  $^1\text{H}$ NMR spectra of methacryloyl gelatin and gelatin in  $\text{D}_2\text{O}$  (B) FTIR spectra of gelatin, hyaluronic acid, hyaluronan dialdehyde and gelatin-hyaluronan dialdehyde Schiff's polymer (C)  $^1\text{H}$  NMR spectra of gelatin, hyaluronic acid (HA), HDA and Gel-HDA in  $\text{D}_2\text{O}$ .



**Figure 2.** Mechanical properties of GelMA and IPN hydrogels containing  $0.1 \text{ mg ml}^{-1}$  LAP and photocrosslinked for 1 min. (A) Stress–strain graphs of GelMA and different IPNs and (B) compressive modulus obtained by the linear curve fitting from 0%–10% strain region.



**Figure 3.** Determination of (A) the shear equilibrium modulus (at  $20^\circ\text{C}$ ,  $10 \text{ rad s}^{-1}$ , and 1% strain) and (B) mechanical spectra at  $20^\circ\text{C}$  and 1% strain of GelMA 10 w/v% and Gel-HDA/GelMA IPN (gelatin 10% (w/v), HDA 5% (w/v) and GelMA 10% (w/v)). (C) Temperature dependence of the dynamic mechanical moduli of GelMA 10% (w/v) and Gel-HDA/GelMA IPN physical hydrogels.

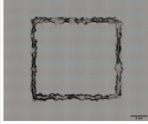
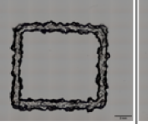
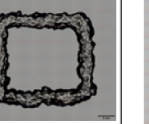

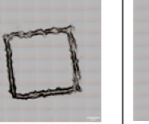


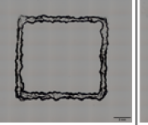
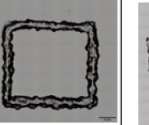

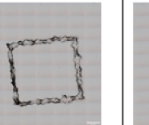
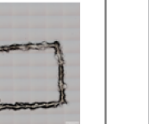
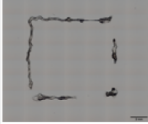
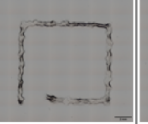

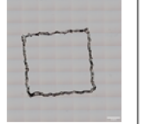
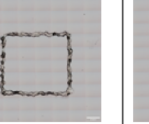

Representative graphs of the stress–strain curve of different IPN samples are shown in figure 2(A). The compressive modulus of GelMA was determined to be  $116.7 \pm 14.80 \text{ KPa}$ . This is significantly higher than the reported values [33–35]. This could be due to the higher methacryloyl substitution resulting in a higher crosslinking density. The Schiff's base linkage in Gel-HDA network is a dynamic covalent linkage, and the incorporation of Gel-HDA network in the IPN sample resulted in the decline of mechanical properties. As the concentration of Gel-HDA network increases, the compressive modulus decreases and reaches a minimum value of  $20.6 \pm 2.48 \text{ KPa}$  (figure 2(B)). Gel-HDA alone is not able to maintain its shape for mechanical testing.

### 3.4. Rheology

To analyze the rheological properties of the Gel-HDA/GelMA IPN hydrogel precursor, small-amplitude shear rheometry was used to perform time sweep, frequency sweep and temperature sweep tests. In the time sweep test, the storage and the loss modulus ( $G'$  and  $G''$ ) were recorded for 2 h at  $20^\circ\text{C}$  and an angular frequency of  $10 \text{ rad s}^{-1}$  to determine the equilibrium modulus of the hydrogels. The Gel-HDA/GelMA IPN hydrogel was found to be a stronger hydrogel than GelMA, with the values of 1000 and 600 Pa respectively (figure 3(A)). Moreover, the Gel-HDA/GelMA IPN hydrogel showed faster physical gelation kinetics, which in turn, can reduce the residence time of encapsulated cells prior to printing. The



(A)

Plunger velocity Feed rate	GelMA			IPN		
	0.05 mm/s	0.1 mm/s	0.2 mm/s	0.05 mm/s	0.1 mm/s	0.2 mm/s
5 mm/s	 Pr = 1.12	 Pr = 1.14	 Pr = 1.09	 Pr = 1.08	 Pr = 1.09	 Pr = 1.14
10 mm/s	 Broken	 Pr = 1.07	 Pr = 1.11	 Pr = 1.13	 Pr = 1.14	 Pr = 1.10
15 mm/s	 Broken	 Broken	 Broken	 Pr = 1.07	 Pr = 1.14	 Pr = 1.14

**Figure 4.** Assessment of printability. (A) GelMA and IPN samples were extruded through 27 G nozzle to form a square-shaped construct by applying different plunger velocity and feed rates. Pr values showed as an average of three replicates. (B) Printability of GelMA and Gel-HDA/GelMA IPN hydrogels printed at room temperature. The GelMA ink was incubated in the fridge at 4 °C for 20 min to attain required viscosity for printing. Images showing CAD designs on the top and the corresponding 3D printed shapes such as grid, stacked hollow cylinder and alphabets 'S', 'B' and 'E' (10 × 10 mm, the distance between two strands 2 mm, layer height 0.2 mm) as five layers constructs at the bottom. Scale bar is 5 mm.

frequency sweep test (figure 3(B)) showed constant values of  $G'$  at low angular frequencies, indicating the existence of a sample-spanning network structure. The predominance of  $G'$  over  $G''$  over the entire angular frequency range is a characteristic signature of a solid-like gel behavior. The sol-gel transition temperature of the hydrogels was measured via temperature sweep measurements (10 °C–40 °C and 40 °C–10 °C) in the linear regime at a low heating rate of 1 °C min<sup>-1</sup> (figure 3(C)). The results demonstrated that the proposed IPN-hydrogel has a higher gelation temperature (30 °C) than GelMA (27 °C).

### 3.5. 3D printing of Gel-HDA/GelMA IPN constructs

A semi-quantitative evaluation of the printability of GelMA and IPN biomaterial inks was performed by calculating the printability parameter (Pr) for each feed rate-plunger velocity combination (figure 4(A)). According to the literature, the Pr value in the range of 0.9–1.1 is considered as a good filament morphology [25]. Before printing, GelMA ink had to be pre-conditioned at 4 °C to attain required viscosity for printing, while the IPN ink attained the required viscosity by pre-conditioning at room temperature for the same time. Based on the analysis, for GelMA, a feed rate of 10 mm s<sup>-1</sup> and plunger velocity of 0.1 mm s<sup>-1</sup> and for IPN, a feed rate of

5 mm s<sup>-1</sup> and plunger velocity of 0.05 mm s<sup>-1</sup> are the optimum parameters for printing at room temperature (~21 °C). Furthermore, considering resolution as the minimum distance of two distinguishable printed strands, the width of the printed lines was calculated to determine the optimum parameters for printing. Among GelMA samples, the best resolution was obtained for the samples printed with a feed rate of 15 mm s<sup>-1</sup>, and a plunger velocity of 0.05 mm s<sup>-1</sup>, resulting in an average width of 0.26 mm and the best resolution for the IPN sample was obtained with the same parameters resulting in an average width of 0.32 mm. The calculations show the line width for GelMA to be narrower at these conditions. However, the GelMA squares printed with these conditions were broken, while IPN samples resulted in near perfect squares.

Different shapes (grid, stacked hollow cylinder, and alphabets) were patterned using 3D printing at room temperature. The physical crosslinking of the IPN precursors enabled shape fidelity of the constructs while printing, and the UV crosslinking ensured their long-term stability. The images of the constructs (figure 4(B)) were taken immediately after printing. Both GelMA (pre-conditioned ink) and IPN inks were printable at room temperature by applying respective printing parameters. The advantage of IPN ink over GelMA (DS ~100%) is the possibility

(B)

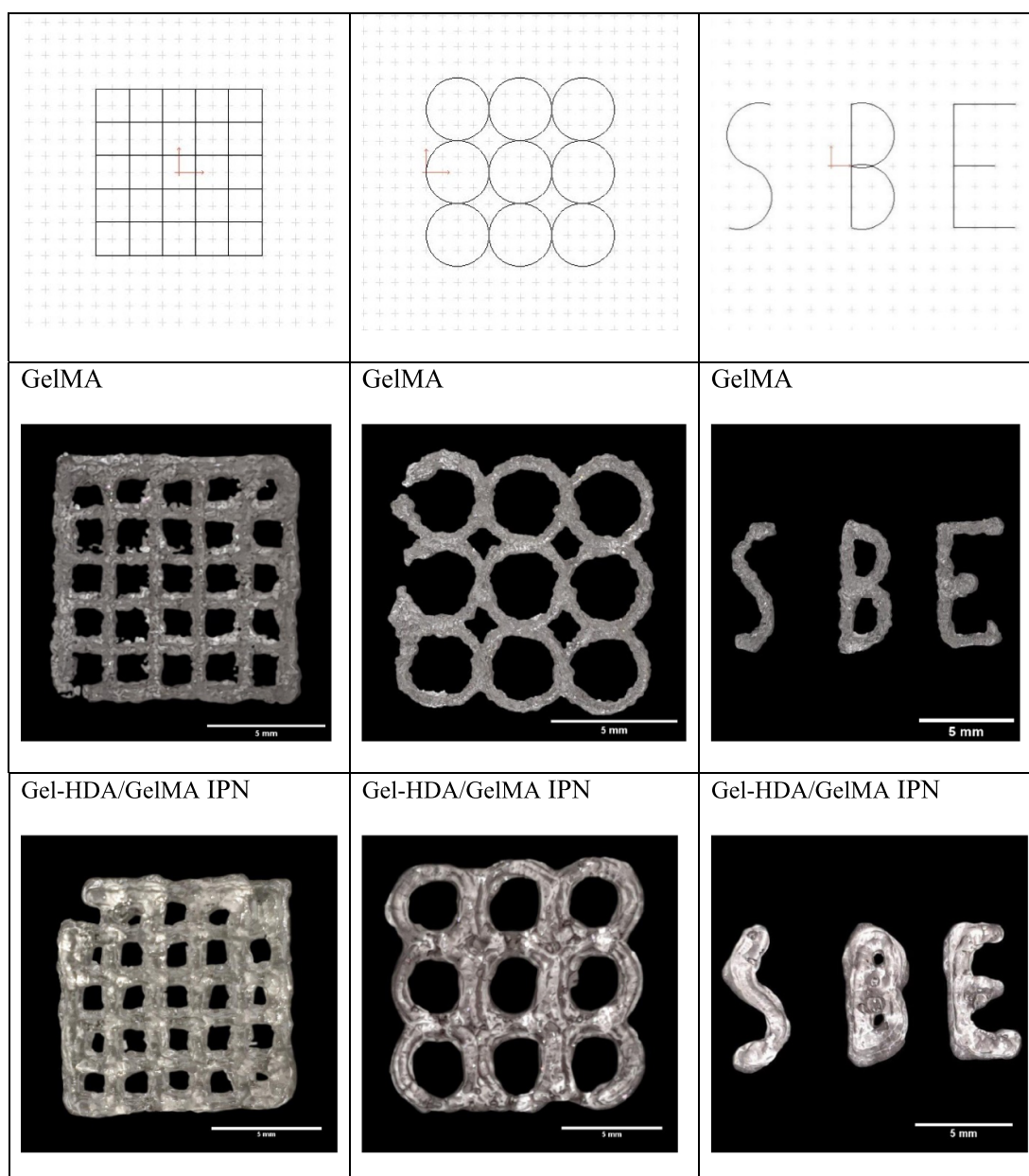


Figure 4. (Continued.)

of relatively rapid sol-gel transition at room temperature.

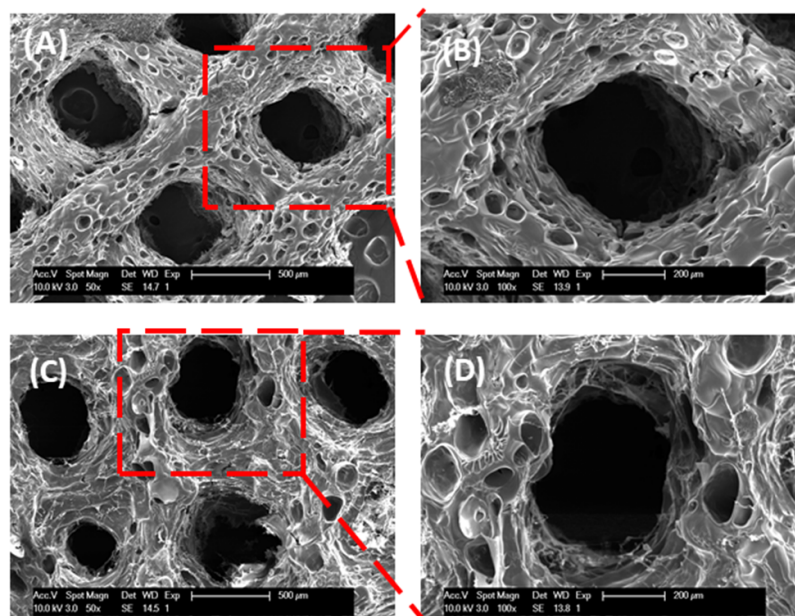
### 3.6. Surface morphology of the 3D printed construct

SEM images of GelMA and IPN 3D printed grid construct showed a porous morphology with an average pore size of approximately 54  $\mu\text{m}$  and 131  $\mu\text{m}$  respectively. However, the purpose of this measurement is to compare the difference among GelMA and IPN and not the exact values, as the exact value also depends on preparation procedure which includes freeze drying. The higher magnification of figures 5(A) and (C) are shown in figures 5(B) and (D), respectively. The large pores ( $\sim 500 \mu\text{m}$ ) present

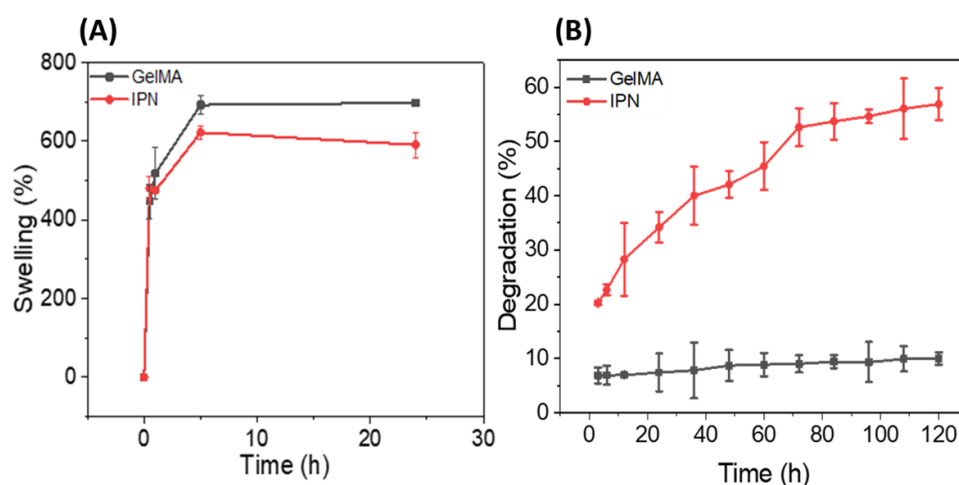
in figures 5(A)–(D) are the pores resulting from the designed grid construct. The pore size of GelMA construct is significantly lower than the reported values [34, 36]. This can be attributed to the 100% methacryloyl functionalization of gelatin resulting in a higher degree of crosslinking, which is known to have a significant effect on hydrogel pore size [37]. It is anticipated that the microporous network of the IPN hydrogel and the grid construct design may enhance cell growth and cell proliferation as it can easily transport nutrients and other metabolites into the construct.

### 3.7. Swelling and degradation behaviour

Swelling behaviour of GelMA and IPN samples were analyzed by measuring the difference in weight of the



**Figure 5.** Scanning electron microscopy images of 3D printed (A) and (B) GelMA and (C) and (D) Gel-HDA/GelMA IPN hydrogels (two layer construct, the distance between the strands = 1 mm), presenting the effect of the interpenetrated network structure on the pore size and surface morphology of GelMA. The scale bars of (A) and (C) are 500  $\mu\text{m}$  and (B) and (D) are 200  $\mu\text{m}$  respectively.

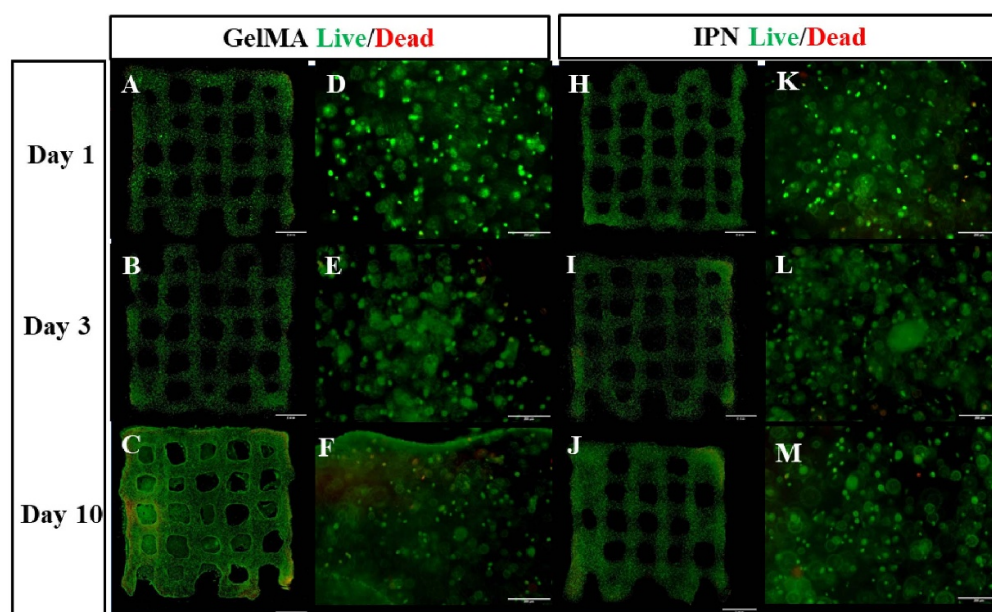


**Figure 6.** (A) Swelling and (B) degradation behaviors of methacryloyl gelatin and IPN hydrogel at 37 °C. The swelling studies were performed in phosphate buffer (pH 7.4) and the degradation studies were performed in DMEM.

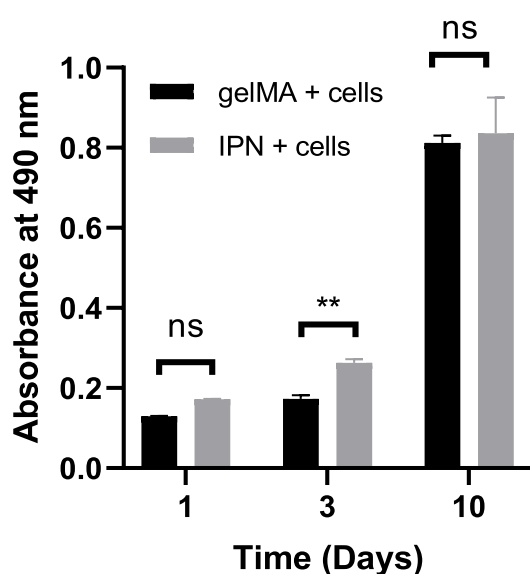
samples at different incubation periods in PBS (pH 7) at 37 °C under static conditions. The swelling behaviour shown in figure 6(A) demonstrated a higher swelling rate for GelMA than IPN due to the presence of higher crosslinking and interpenetrated network structure in the IPN [38]. Both GelMA and IPN samples reached an equilibrium swelling state after 5 h and after that, a slight decrease in the percentage of swelling was observed for IPN. This could be due to the faster degradation of IPN samples caused by the weaker 3D network structure of Gel-HDA component. The biodegradability of the hydrogel has a

significant role in the tissue regeneration as it can provide sufficient room for tissue ingrowth when implanted into the body. Figure 6(B) demonstrated that GelMA (10%) could maintain its network stability in DMEM during the 5 days study whereas the incorporation of Gel-HDA network and a lower GelMA concentration in the IPN hydrogel has highly increased the degradation rate of the IPN hydrogel. This can be attributed to a combination of the hydrolytic degradation of the gelMA, exacerbated by polymer mass loss caused by the relatively weaker dynamic covalent links of the Gel-HDA network.

(A)



(B)



**Figure 7.** (A) Fluorescence imaging of MC3T3 cells encapsulated in GelMA (A, B and C are 4× magnification (scale bar 2 mm) and D, E and F are corresponding 10× magnification (scale bar 200 μm)) and IPN (G, H and I are 4× magnification (scale bar 2 mm), J, K and L are corresponding 10× magnification (scale bar 200 μm)) hydrogel, bioprinted and visualized after 1, 3 and 10 days *in vitro* culture. Live cells were visualized by staining with calcein-green and dead cells with ethidium homo dimer-red. (B) Quantification of cell proliferation in GelMA and IPN hydrogel until 10 days by MTS assay (\*\*  $p \leq 0.01$ ).

### 3.8. *In vitro* cell viability and cell proliferation

The *in vitro* viability of MC3T3 cells encapsulated in the bioprinted GelMA and IPN constructs was evaluated by using a live/dead assay after 1, 3 and 10 days (figure 7(A)). The high viability of MC3T3-E1 cells in the bioprinted construct after day 1 indicated a high cell survival after printing. Similar to GelMA,

the cells were able to proliferate and attach well inside the bioprinted Gel-HDA/GelMA IPN construct due to the favorable material properties. Only a few dead cells were observed (visible in red in the enlarged image). As shown in figure 7(A), MC3T3-E1 cells encapsulated in both constructs displayed cell proliferation. The metabolic activity of the cells in GelMA



and IPN constructs increased significantly within 10 days of *in vitro* culture ( $P \leq 0.0001$ ), demonstrating proliferation within this time period (figure 7(B)). However, no noticeable differences were observed among the GelMA and IPN samples analyzed at the beginning and end of the study due to the same number of encapsulated cells in the beginning and complete infiltration of the constructs by the cells at the end. However, during the study (day 3) the cell proliferation seemed to be faster in IPN constructs which could be attributed to global stress relaxation of IPN hydrogels caused by the presence of dynamic covalent linkage between gelatin and HDA facilitating cell migration within the construct.

## 4. Conclusion

The present study reports the design of an IPN hydrogel combining the beneficial properties of gelatin and a natural polysaccharide, hyaluronic acid, for its potential application as a bioink for tissue regeneration. The less stable HA was covalently cross-linked with gelatin and interpenetrated into a GelMA polymer network enhancing the retention of the HA in the IPN network. Furthermore, the higher sol-gel transition temperature and faster gelation of Gel-HDA/GelMA IPN hydrogel, allowed for 3D bioprinting at room temperature. An *in vitro* assessment of the cell viability and cell metabolic activity of the cells encapsulated in the bioprinted constructs demonstrated that the hydrogel constructs provided a suitable environment for the cell survival and proliferation over 10 days. These results along with the tunable mechanical behavior enabled the preparation of novel cell-laden bioinks for diverse tissue engineering applications.

## Data availability statement

The data that support the findings of this study are available upon reasonable request from the authors.

## Acknowledgements

The authors acknowledge funding from European Research Council (ERC) under the European Union's Horizon 2020 research and innovation programme (Grant Agreement No. 772418). R A acknowledges DST INSPIRE Faculty award (DST/INSPIRE/04/2016/000482) for financial support. M S A acknowledges Research Council of KU Leuven Grant No. (C24/18/068). The current address of R A is Materials Research and Technology, Luxembourg Institute of Science and Technology, 5 Avenue des Hauts Fourneaux, Esch/Alzette L-4362, Luxembourg.

## Conflict of interest

None.

## ORCID iD

Resmi Anand  <https://orcid.org/0000-0001-6078-3244>

## References

- [1] Murphy S V and Atala A 2014 3D bioprinting of tissues and organs *Nat. Biotechnol.* **32** 773–85
- [2] Gungor-Ozkerim P S, Inci I, Zhang Y S, Khademhosseini A and Dokmeci M R 2018 Bioinks for 3D bioprinting: an overview *Biomater. Sci.* **6** 915–46
- [3] Ozbolat I T and Hospodiuk M 2016 Current advances and future perspectives in extrusion-based bioprinting *Biomaterials* **76** 321–43
- [4] Amorim P A, d'Ávila M A, Anand R, Moldenaers P, Van Puyvelde P and Bloemen V 2021 Insights on shear rheology of inks for extrusion-based 3D bioprinting *Bioprinting* **22** e00129
- [5] Stanton M M, Samitier J and Sánchez S 2015 Bioprinting of 3D hydrogels *Lab Chip* **15** 3111–5
- [6] Chimene D, Kaunas R and Gaharwar A K 2020 Hydrogel bioink reinforcement for additive manufacturing: a focused review of emerging strategies *Adv. Mater.* **32** 1902026
- [7] Liu W *et al* 2017 Extrusion bioprinting of shear-thinning gelatin methacryloyl bioinks *Adv. Healthcare Mater.* **6** 1601451
- [8] Yue K, Trujillo-de Santiago G, Alvarez M M, Tamayol A, Annabi N and Khademhosseini A 2015 Synthesis, properties, and biomedical applications of gelatin methacryloyl (GelMA) hydrogels *Biomaterials* **73** 254–71
- [9] Pepelanova I, Kruppa K, Scheper T and Lavrentieva A 2018 Gelatin-methacryloyl (GelMA) hydrogels with defined degree of functionalization as a versatile toolkit for 3D cell culture and extrusion bioprinting *Bioengineering* **5** 55
- [10] Hoch E, Hirth T, Tovar G E M and Borchers K 2013 Chemical tailoring of gelatin to adjust its chemical and physical properties for functional bioprinting *J. Mater. Chem. B* **1** 5675
- [11] Gao Q *et al* 2019 3D printing of complex GelMA-based scaffolds with nanoclay *Biofabrication* **11** 035006
- [12] Sultan S and Mathew A P 2018 3D printed scaffolds with gradient porosity based on a cellulose nanocrystal hydrogel *Nanoscale* **10** 4421–31
- [13] Fares M M, Shirzaei Sani E, Portillo Lara R, Oliveira R B, Khademhosseini A and Annabi N 2018 Interpenetrating network gelatin methacryloyl (GelMA) and pectin-g-PCL hydrogels with tunable properties for tissue engineering *Biomater. Sci.* **6** 2938–50
- [14] Zhou M, Lee B H, Tan Y J and Tan L P 2019 Microbial transglutaminase induced controlled crosslinking of gelatin methacryloyl to tailor rheological properties for 3D printing *Biofabrication* **11** 025011
- [15] Schipani R, Scheurer S, Florentin R, Critchley S E and Kelly D J 2020 Reinforcing interpenetrating network hydrogels with 3D printed polymer networks to engineer cartilage mimetic composites *Biofabrication* **12** 035011
- [16] Matricardi P, Di Meo C, Coviello T, Hennink W E and Alhaique F 2013 Interpenetrating polymer networks polysaccharide hydrogels for drug delivery and tissue engineering *Adv. Drug Deliv. Rev.* **65** 1172–87
- [17] Hemshekhar M, Thushara R M, Chandranayaka S, Sherman L S, Kemparaju K and Girish K S 2016 Emerging roles of hyaluronic acid bioscaffolds in tissue engineering and regenerative medicine *Int. J. Biol. Macromol.* **86** 917–28
- [18] Misra S, Hascall V C, Markwald R R and Ghatak S 2015 Interactions between hyaluronan and its receptors (CD44, RHAMM) regulate the activities of inflammation and cancer *Front. Immunol.* **6** 1–31
- [19] Murakami T, Otsuki S, Okamoto Y, Nakagawa K, Wakama H, Okuno N and Neo M 2019 Hyaluronic acid promotes proliferation and migration of human meniscus



- cells via a CD44-dependent mechanism *Connect. Tissue Res.* **60** 117–27
- [20] Abatangelo G, Vindigni V, Avruscio G, Pandis L and Brun P 2020 Hyaluronic acid: redefining its role *Cells* **9** 1743
- [21] Pescosolido L, Schuurman W, Malda J, Matricardi P, Alhaque F, Coviello T, van Weeren P R, Dhert W J A, Hennink W E and Vermonden T 2011 Hyaluronic acid and dextran-based semi-IPN hydrogels as biomaterials for bioprinting *Biomacromolecules* **12** 1831–8
- [22] Lou J, Stowers R, Nam S, Xia Y and Chaudhuri O 2018 Stress relaxing hyaluronic acid-collagen hydrogels promote cell spreading, fiber remodeling, and focal adhesion formation in 3D cell culture *Biomaterials* **154** 213–22
- [23] Deng Y, Ren J, Chen G, Li G, Wu X, Wang G, Gu G and Li J 2017 Injectable *in situ* cross-linking chitosan-hyaluronic acid based hydrogels for abdominal tissue regeneration *Sci. Rep.* **7** 2699
- [24] Shirahama H, Lee B H, Tan L P and Cho N-J 2016 Precise tuning of facile one-pot gelatin methacryloyl (GelMA) synthesis *Sci. Rep.* **6** 31036
- [25] Ouyang L, Yao R, Zhao Y and Sun W 2016 Effect of bioink properties on printability and cell viability for 3D bioplotting of embryonic stem cells *Biofabrication* **8** 035020
- [26] Schindelin J et al 2012 Fiji: an open-source platform for biological-image analysis *Nat. Methods* **9** 676–82
- [27] Pandit A H, Mazumdar N and Ahmad S 2019 Periodate oxidized hyaluronic acid-based hydrogel scaffolds for tissue engineering applications *Int. J. Biol. Macromol.* **137** 853–69
- [28] Peach R, Hollenbaugh D, Stamenkovic I and Aruffo A 1993 Identification of hyaluronic acid binding sites in the extracellular domain of CD44 *J. Cell Biol.* **122** 257–64
- [29] Zhu H, Mitsuhashi N, Klein A, Barsky L W, Weinberg K, Barr M L, Demetriou A and Wu G D 2006 The role of the hyaluronan receptor CD44 in mesenchymal stem cell migration in the extracellular matrix *Stem Cells* **24** 928–35
- [30] Weng L, Pan H and Chen W 2008 Self-crosslinkable hydrogels composed of partially oxidized hyaluronan and gelatin: invitro andin vivo responses *J. Biomed. Mater. Res. A* **85A** 352–65
- [31] Su W-Y, Chen Y-C and Lin F-H 2010 Injectable oxidized hyaluronic acid/adipic acid dihydrazide hydrogel for nucleus pulposus regeneration *Acta Biomater.* **6** 3044–55
- [32] Zhou X, Zhu W, Nowicki M, Miao S, Cui H, Holmes B, Glazer R I and Zhang L G 2016 3D bioprinting a cell-laden bone matrix for breast cancer metastasis study *ACS Appl. Mater. Interfaces* **8** 30017–26
- [33] Yin J, Yan M, Wang Y, Fu J and Suo H 2018 3D bioprinting of low-concentration cell-laden gelatin methacrylate (GelMA) bioinks with a two-step cross-linking strategy *ACS Appl. Mater. Interfaces* **10** 6849–57
- [34] Noshadi I et al 2017 *In vitro* and *in vivo* analysis of visible light crosslinkable gelatin methacryloyl (GelMA) hydrogels *Biomater. Sci.* **5** 2093–105
- [35] Beck E C, Barragan M, Tadros M H, Gehrke S H and Detamore M S 2016 Approaching the compressive modulus of articular cartilage with a decellularized cartilage-based hydrogel *Acta Biomater.* **38** 94–105
- [36] Krishnamoorthy S, Noorani B and Xu C 2019 Effects of encapsulated cells on the physical–mechanical properties and microstructure of gelatin methacrylate hydrogels *Int. J. Mol. Sci.* **20** 5061
- [37] Zhao X, Lang Q, Yildirimer L, Lin Z Y, Cui W, Annabi N, Ng K W, Dokmeci M R, Ghaemmaghami A M and Khademhosseini A 2016 Photocrosslinkable gelatin hydrogel for epidermal tissue engineering *Adv. Healthcare Mater.* **5** 108–18
- [38] Suo H, Zhang D, Yin J, Qian J, Wu Z L and Fu J 2018 Interpenetrating polymer network hydrogels composed of chitosan and photocrosslinkable gelatin with enhanced mechanical properties for tissue engineering *Mater. Sci. Eng. C* **92** 612–20